The Journal of Chemical Physics

Static permittivity of environmentally relevant low-concentration aqueous solutions of $NaCl$, $NaNO_3$, and Na_2SO_4

Cite as: J. Chem. Phys. **153**, 014503 (2020); https://doi.org/10.1063/1.5144301
Submitted: 03 January 2020 . Accepted: 09 June 2020 . Published Online: 01 July 2020

Amin Gorji, and Nicola Bowler

The Journal of Chemical Physics ARTICLE scitation.org/journal/jcp

Static permittivity of environmentally relevant low-concentration aqueous solutions of NaCl, $NaNO_3$, and Na_2SO_4

Cite as: J. Chem. Phys. 153, 014503 (2020); doi: 10.1063/1.5144301
Submitted: 3 January 2020 • Accepted: 9 June 2020 •
Published Online: 1 July 2020

Amin Gorji[1,2] and Nicola Bowler[1,2,3,a)]

AFFILIATIONS

[1] Department of Electrical and Computer Engineering, Iowa State University, Ames, Iowa 50011, USA
[2] Center for Nondestructive Evaluation, Iowa State University, Ames, Iowa 50011, USA
[3] Department of Materials Science and Engineering, Iowa State University, Ames, Iowa 50011, USA

[a)] **Author to whom correspondence should be addressed:** nbowler@iastate.edu

ABSTRACT

In this paper, the result of a systematic study and molecular mechanisms governing the dielectric spectra of aqueous solutions of NaCl, $NaNO_3$, and Na_2SO_4 with environmentally relevant concentrations (~mmol/l) are presented, for frequencies from 200 MHz up to 20 GHz and at temperature 25.00 ± 0.01 °C. The measured spectra were fitted with a Debye relaxation model using a non-linear, weighted, least-squares analysis. Conductivity was measured independently to reduce uncertainty in obtaining other parameters by spectral fitting. Careful experimentation provided dielectric data of sufficiently low uncertainty to enable observation of polarization mechanisms that emerge only in the low-concentration regime. The data were fitted by a concentration-dependent parametric model that includes terms accounting for internal depolarizing fields and the solvent dilution effect (mixture relation), the kinetic depolarization effect, the dielectric saturation effect, and the Debye–Falkenhagen effect that accounts for the contribution of ionic atmosphere polarization. It has been shown that, in NaCl and $NaNO_3$ solutions at sufficiently low concentrations, the static permittivity increases due to the Debye–Falkenhagen effect. It has also been shown that, to calculate the number of irrotationally bound water molecules Z_{IB}, the measured static permittivity values should be corrected to account for the contributions of kinetic depolarization and Debye–Falkenhagen effects. Otherwise, unrealistic values of Z_{IB} are obtained. An explanation for the different strengths of the Debye–Falkenhagen effect observed for the different electrolyte solutions, essentially due to the electrophoretic effect and coordination number, is also presented.

I. INTRODUCTION

Excessive amounts of unwanted chemicals and ions flowing into water sources are concerning, for environmental and human health-related reasons. Electrolyte solutions of nitrate (NO_3^-), chloride (Cl^-), and sulfate (SO_4^{2-}) ions in water are among the most common pollutants[1] that can cause serious environmental and human health problems. Understanding the dielectric properties of such electrolytes is of considerable interest, providing information about molecular (polarization) and ionic (charge-transport) dynamics.[2] Dielectric spectroscopy (DS), a technique to measure the complex permittivity, i.e., its complex relative permittivity $\varepsilon(f) = \varepsilon'(f) - j\varepsilon''(f)$, to an applied time-harmonic electric field oscillating with frequency f is a powerful technique for characterizing unique properties of the nature and dynamics of electrolyte solutions.[3] At sufficiently low frequency, DS detects all mechanisms that contribute to the polarization of the sample.[4] As frequency increases, relaxation or resonance events take place at their characteristic frequencies. At frequencies higher than those characteristic frequencies, the contribution of the particular polarization mechanism associated with that relaxation or resonance, to the overall polarization of the sample, is lost. Real relative permittivity $\varepsilon'(f)$ indicates to what extent electrical energy may be stored in the material, while imaginary relative permittivity $\varepsilon''(f)$ indicates the degree

of dissipation of electrical energy (dielectric loss) in the sample, whether by conduction or polarization loss.

The dielectric properties of various moderate- and high-concentration solutions of mono-/bivalent nitrate, chloride, and sulfate-based ions dissolved in water have been characterized in prior works.[5–7] Table I summarizes results of the most recent dielectric studies of sodium-based nitrate, chloride, and sulfate ions. Of note, the dielectric properties of $NaNO_3$(aq) reported by Lileev *et al.*[8] are of very high-concentration samples $c \sim 0.52$ mol/l–8.54 mol/l over five discrete frequencies between 7 GHz and 25 GHz and different temperatures from 10 °C to 40 °C. Wachter *et al.*,[9] however, covered a broad frequency range up to 89 GHz within the concentration range $c \sim 0.05$ mol/l–1.5 mol/l at $T = 25$ °C.

Most of the previous studies, however, did not consider environmentally relevant concentration levels of NaCl(aq), $NaNO_3$(aq), and Na_2SO_4(aq), which are on the order of millimoles per liter. Conclusions drawn from previous studies on moderate- and high-concentration solutions do not provide a picture of the dielectric properties in the low-concentration regime. A need for dielectric data for low concentrations of these ions has arisen in the context of a need for real-time monitoring of contaminant ions in water sources.[15] In addition, the data obtained for low concentrations should be of higher accuracy than are currently available in the literature because the small variations in ε' and ε'' in low-concentration solutions may otherwise be concealed by the experimental uncertainties of ε' and ε''.

In this paper, the dielectric properties of environmentally relevant, low-concentration, aqueous solutions of NaCl, $NaNO_3$, and Na_2SO_4 are characterized in a well-controlled laboratory experiment. In Sec. II, the details of the experimental setup to perform dielectric spectroscopy over the frequency range 200 MHz to 20 GHz and to measure specific conductivity are presented. Methods of extracting meaningful permittivity parameters from the dielectric spectra are also presented in Sec. II. In Sec. III, a semi-empirical model to represent the static permittivity, ε_{dc}, of multivalent electrolyte systems is introduced. This concentration-dependent model expresses the contributions of distinct mechanisms to static permittivity in the low-concentration regime. Section IV is devoted to results and discussion, and the paper is drawn to conclusion in Sec. V.

II. EXPERIMENTAL METHOD AND DATA ANALYSIS

The details of the measurement instruments and the procedure are explained in Ref. 16. In summary, dielectric experiments were performed at 200 MHz to 20 GHz using a SPEAG 3.5 mm open-ended coaxial probe and vector network analyzer (VNA). In addition, the specific conductivity σ was measured separately using a conductivity meter. For concentrations of ionic solutions corresponding to specific conductivity greater than 500 μS/cm, however, σ was treated as an additional fitting parameter. The temperature was held at 25.00 ± 0.01 °C during the experiment. Three sets of agriculturally relevant ionic aqueous solutions were prepared, and 14 concentrations c of each (including deionized water as zero concentration) were tested: (i) aqueous sodium chloride (NaCl) with concentration ranging from $c = 0$ mmol/l to 11.26 mmol/l, (ii) aqueous sodium nitrate ($NaNO_3$) with $c = 0$ mmol/l–17.83 mmol/l, and (iii) aqueous sodium sulfate (Na_2SO_4) with $c = 0$ mmol/l–12.45 mmol/l. These ranges, despite being different, correspond to 0 mg/l–400 mg/l concentration of sodium chloride as chloride (NaCl–Cl), sodium nitrate as nitrogen ($NaNO_3$–N), and sodium sulfate as sulfur (Na_2SO_4–S), which is the commonly represented unit in agricultural societies. Measurements were made on samples of increasing concentration, by successive titration of a pre-calculated volume of each stock electrolyte into a specified volume of deionized water. This procedure eliminates the need for cleaning and refilling the probe between successive measurements; otherwise, a significant error would have been introduced to the measured data due to mechanical disturbances from cleaning and touching the probe.

Combining the frequency dependence of polarization $\varepsilon'(f)$ and energy dissipation $\varepsilon''(f)$ of an electrolyte solution in response to an applied electric field, the total complex relative permittivity $\varepsilon_T(f)$ can be written as

$$\begin{aligned}\varepsilon_T(f) &= \varepsilon'(f) - j\varepsilon''(f)\\ &= \varepsilon'(f) - j\left[\varepsilon_d''(f) + \frac{\sigma}{2\pi\varepsilon_0 f}\right],\end{aligned} \tag{1}$$

where the energy dissipation component $\varepsilon''(f)$ is composed of dipolar loss $\varepsilon_d''(f)$ and specific conductivity σ (dc conductivity) terms. The measured dielectric spectra (total complex relative permittivity)

TABLE I. A summary of most recent previous studies of dielectric properties for aqueous (aq) solutions of NaCl, $NaNO_3$, and Na_2SO_4. The table summarizes the studied range of concentration (c), frequency (f), and temperature (T).

References	Sample	c (mol/l)	f (GHz)	T (°C)
Nörtemann *et al.*[10]	NaCl(aq)	0.05–0.6	0.02–40	20
Buchner *et al.*[11]	NaCl(aq)	0.1–5	0.2–20	5, 20, 25, 35
Levy *et al.*[12]	NaCl(aq)	0.1–1	0.5–50	25
Lileev *et al.*[8]	$NaNO_3$(aq)	0.52–8.54	7–25[a]	10, 15, 25, 35, 40
Wachter *et al.*[9]	$NaNO_3$(aq)	0.05–1.5	0.2–89	25
Barthel *et al.*[13]	Na_2SO_4(aq)	0.1–1	0.95–89	25
Buchner *et al.*[14]	Na_2SO_4(aq)	0.025–1.6	0.95–89	25

[a]Measured at five discrete frequencies.

for three examples of NaCl, $NaNO_3$, and Na_2SO_4 with approximately the same concentration, $c \sim 7$ mmol/l, are presented in Fig. 1. The plotted data are the average of 10 recorded spectra for each aqueous solution. The loss spectra $\varepsilon''(f)$ are also decomposed into the contributions from the conductivity term $\sigma/2\pi f\varepsilon_0$, where σ is the specific conductivity, and dipolar loss $\varepsilon_d''(f)$. The fitting procedure of dielectric spectra for low concentrations of solute for which the dielectric spectrum varies only slightly from that of pure water is described in Ref. 16. Within the frequency range under consideration, the corrected complex relative permittivity $\varepsilon_c(f) = \varepsilon'(f) - j\varepsilon_d''(f)$ (conductivity contribution is subtracted from ε'') can be approximated by a single-term Debye relaxation model as

$$\varepsilon_{Debye}(f) = \varepsilon'_{Debye}(f) - j\varepsilon''_{Debye}(f) = \varepsilon_\infty + \frac{\varepsilon_{dc} - \varepsilon_\infty}{1 + j2\pi f\tau}. \quad (2)$$

where ε_{dc} is the static permittivity, ε_∞ is the permittivity at a frequency well above that of the relaxation frequency f_r, and $\tau = 1/(2\pi f_r)$ is the relaxation time. The reason for correcting for the specific conductivity is to subtract the ionic migration (i.e., conductivity) contribution from $\varepsilon''(f)$ in order to deal separately with dipolar polarizations represented by $\varepsilon_d''(f)$. Among other relaxation models,[17] the dielectric spectra of the present electrolyte solutions can be best described by a single-term Debye relaxation model in the low-concentration range (~mmol/l). In principle, ε_∞ is identified as the plateau reached by $\varepsilon'(f)$ when all polarization contributions associated with intermolecular dynamics are no longer effective.[7] Thus, ε_∞ reflects only contributions from intramolecular polarizability that could be obtained from dielectric spectroscopy in the terahertz region.[18] Since this is far above our upper limit of measured frequency, ε_∞ was treated as an additional fitting parameter in Ref. (2). This treatment results in slightly increased values of the reduced variance of the fit, s^2, but also produces a smoother progression of the fitting parameters as a function of concentration. An alternative approach in which the value of ε_∞ is fixed during the fitting procedure, depending on particular scenarios, has also been reported in the literature.[10,11]

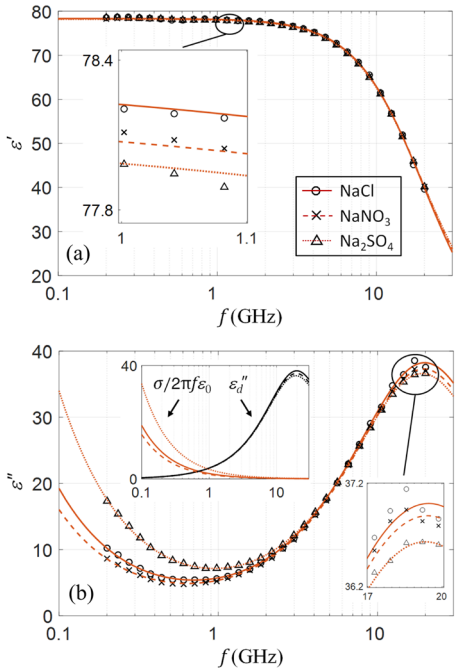

FIG. 1. Dielectric dispersion $\varepsilon'(f)$ (a) and loss $\varepsilon''(f)$ (b) spectra of aqueous solutions of NaCl with $c = 7.052$ mmol/l; $NaNO_3$ with $c = 7.139$ mmol/l; and Na_2SO_4 with $c = 7.797$ mmol/l at $T = 25\,^\circ$C. The symbols represent the measured permittivity data. The lines represent the fitted curves (single-term Debye relaxation model). The contributions due to the conductivity term ($\sigma/2\pi f\varepsilon_0$) and the dipolar relaxation process $\varepsilon_d''(f)$ are shown separately in the inset of (b). The plotted data are the average of 10 recorded spectra for each aqueous solution. The corresponding uncertainties for each measured data are calculated in Ref. 16.

A simultaneous, non-linear, weighted, unconstrained, least-squares analysis to minimize the residuals χ^2 was performed, based on the Gauss–Marquardt algorithm.[16,19] The benefit of weighted least-squares analysis is that the influence of those data points with higher uncertainties is reduced in minimizing the sum of squares, by giving weights that are inversely proportional to the uncertainty attached to each data point. A careful analysis of the measurement uncertainty is necessary for reliable interpretation of measurement data in general and is particularly important in this case concerning the dielectric properties of electrolyte solutions at low concentrations. The measurement uncertainty that may limit the precision and accuracy of the measurement result derives from random fluctuations of replicate measurements (due to VNA noise, temperature fluctuations, thermoelectric effects, and electromagnetic interference) and from systematic errors (due to non-ideal probe dimensions, imperfect instrument calibration, calibration of the probe, and cable phase instability) that influence each result in a similar way. Smaller uncertainties of the fitting parameters for low-concentration aqueous solutions can be achieved by calibrating against a reference liquid (deionized water), which has very similar properties to the samples being measured (excluding the conductivity contribution in ε''). In this work, the combined standard uncertainties of the measured dielectric spectra at each frequency, $u_c'(f_i)$ and $u_c''(f_i)$, were calculated in accordance with the established "Guide to the Expression of Uncertainty in Measurement (GUM)" guideline.[20] The uncertainty of the fitting parameters $u(\varepsilon_{dc})$, $u(\tau)$, and $u(\varepsilon_\infty)$, which returned 68% confidence interval, was calculated via Monte Carlo (MC) modeling.[21] Considering the fact that the value of uncertainties for fitting parameters will be used in calculating uncertainties of other parameters (such as the number of irrotationally bound water molecules Z_{IB}), a larger uncertainty will propagate along the calculation and may obscure possible trends in estimated values. As a result, in this work, one standard deviation (coverage factor 1 that is equivalent to 68% confidence interval) is chosen to report the uncertainty.[20] The algorithm to calculate the uncertainties is not possible with proprietary software that came with the SPEAG 3.5 mm probe. All the measurements and calculations for estimating the uncertainties were implemented in-house throughout this work with the details provided in our previous work.[16]

III. MODELING STATIC PERMITTIVITY

The static permittivity ε_{dc} gives insight into possible polarization mechanisms present at the molecular level of electrolyte

solutions. At an ideal zero frequency in which the applied electric field is constant, besides the thermal agitations of molecules, all dipolar moments in the solution tend to align with the direction of the field, thus contributing to the total polarization $\varepsilon'(f = 0) = \varepsilon_{dc}$. At zero concentration, i.e., for deionized water, the value $\varepsilon_{dc}(c = 0) = \varepsilon^0_{dc}$ can be attributed to the total number of water molecules that could align with the applied field. Water molecules, due to the electric charge distribution of their electronic orbitals, form an almost tetrahedrally structured hydrogen-bond (H-bond) network[22] or are "free," i.e., are not H-bonded. The ensemble of water molecules aligned with the applied field are thus either H-bonded water molecules or free water molecules. Buchner *et al.*[23] demonstrated experimentally the existence of a dominant relaxation process in water centered on ~18 GHz at $T = 25\,^{\circ}\mathrm{C}$, which is generally attributed to the kinetics of H-bonded (bulk) water molecules, and a weaker high-frequency relaxation process at around ~120 GHz due to rotational diffusion of free (single) water molecules. Adding ionic solute to water, to form a solution, the behavior of $\varepsilon_{dc}(c)$ depends on the contribution of different mechanisms emerging with respect to the characteristics of the particular ions, including solute–solvent, solute–solute, and solvent–solvent interactions. Another mechanism observable at low concentrations of ionic solute is known as the Debye–Falkenhagen (DF) effect,[24] which is an induced polarization due to charge cloud separations without any molecular association involved in the process.[25] We seek concentration-dependent parametric model to express the behavior of static permittivity over a given concentration range. It is common practice to construct the model by summing contributions of the distinct mechanisms that contribute to static permittivity. These include terms accounting for solvent dilution and internal depolarizing fields, kinetic depolarization effect, dielectric saturation effect, and the Debye–Falkenhagen effect that accounts for the contribution of ionic atmosphere polarization. These contributions are considered in turn in each of the following Subsections III A–III D after which the full model for $\varepsilon_{dc}(c)$ is presented in Subsection III E.

A. Dilution and internal depolarizing field

In order for solute particles to dissolve in water, the positive (cation) and negative (anion) ions must break free from the crystal-lattice structure of the solid. When the ions dissolve in solution, they are surrounded by water molecules. Structure-making ions are small or highly charged ions (sometimes with negative apparent volume) that exert forces to water molecules beyond the first hydration layer. Structure-breaker ions, however, are large ions that do not exert forces to water molecules beyond the first hydration layer.[26] In the case of either type of ion, ion dissociation indeed yields to reduction (dilution) of free and H-bonded water molecules that could otherwise have contributed to the total polarization of the solution. The water molecules form layers of solvation around the ion. Friedman[27] proposed a classification of solvation models into three groups: Hamiltonian, continuous, and chemical. Due to complexity of solutions of the Hamiltonian model and limitations of the continuous model, the chemical models are more extensively used in dielectric studies.[28] In the chemical model, the volume around an ion is divided into two regions. In the exterior region, the solvent molecules are treated as pure solution with zero ion concentration, while in the interior region, they are affected by the presence of ions. In this regard, the early attempts to develop a model of the quantitative dielectric decrement of water due to dissolved ions were made by Sack,[29] Ritson–Hasted,[30] and Glueckauf,[31] where the static permittivity of the solution was found to decrease linearly with ion concentration. In later theories, Pottel's ellipsoidal model[28] that is based on Onsager's spherical model[32] postulates an ellipsoidal zone containing hydration water molecules (water molecules immediately adjacent to a solute particle) together with the solute particle. This ellipsoidal zone is surrounded by a homogeneous host medium with permittivity equal to that of pure water. An additional internal depolarizing field (Lorentz depolarization field),[33] due to electronic polarization of the ion ($\varepsilon_e \sim 2$), is also introduced inside the ellipsoidal zone. The dilution of free and H-bonded water molecules due to solvation, along with the internal depolarizing fields, makes the static permittivity of the solution (effective permittivity) decrease compared to static permittivity of pure water. Although a rigorous theoretical treatment of these mechanisms is not possible, a multitude of mixture relations (effective medium approximations) exist. For ease of calculation, the Maxwell–Wagner relation[34] is employed in this work. The Maxwell–Wagner relation assumes, however, that the permittivity in the direct neighborhood of the ellipsoidal zone (hydration layer) equals that of the pure solvent. In other words, it ignores the long-range interactions between the solute particles and those water molecules outside the solvation layers that are weakly affected by the local fields of the ion charges. For binary mixtures of non-polar solute particles of permittivity ε_e, volume fraction $v(c) = cM/\rho$, where c (mol/l), ρ (g/l), and M (g/mol) are concentration of solute, water density, and solute molecular weight, respectively, and for a background host medium of permittivity ε^0_{dc}, the static permittivity decrement $\delta_{MW}(c)$ according to the Maxwell–Wagner relation is

$$\delta_{MW}(c) = \frac{3v(c)\varepsilon^0_{dc}\left(\varepsilon_e - \varepsilon^0_{dc}\right)}{2\varepsilon^0_{dc} + \varepsilon_e - v(c)\left(\varepsilon_e - \varepsilon^0_{dc}\right)}, \tag{3}$$

where $\varepsilon_e = 2$ is a reasonable approximation in the case of a non-polar spherical solute.[34] Other mixture relations including the Bruggeman relation and the Looyenga relation are formulated in Ref. 35, but the same underlying assumptions hold for them. Further, the Bruggeman relation necessitates solution of a non-linear equation to calculate the static permittivity decrement with respect to solute concentration, adding computational burden to the derivation of a semi-empirical model of the static permittivity.

B. Kinetic depolarization

The measured static permittivity of electrolyte solutions clearly falls below the predictions of mixture relations, because, in an electrolyte solution, the migration of ions under the influence of an external electric field reduces the polarizability of the solvent.[36] In the theoretical framework of the Hubbard–Onsager model,[36] a symmetrically charged impenetrable sphere (the ion) is moving in a viscous, incompressible, polarizable fluid continuum (the solvent).[37] As an ion migrates and sets up a non-uniform flow, according to the laws of hydrodynamics, the surrounding water molecules in the outer regions of the solvation layer are perturbed and tend to rotate in the direction opposite to that promoted by the external field. This

additional polarization deficiency is known as kinetic depolarization $\delta_{KD}(c)$ and is proportional to the specific conductivity $\sigma(c)$ of the solution and the relaxation time τ_s of the solvent. In the case of electrolyte solutions where perfect slip ($p = 2/3$) boundary conditions between the ion surface and solvent continuum are assumed,[11] $\delta_{KD}(c)$ is given by

$$\delta_{KD}(c) = \xi(c)\sigma(c), \tag{4}$$

where $\xi(c)$ is the Hubbard–Onsager coefficient

$$\xi(c) = p\frac{\varepsilon^0_{dc} - \varepsilon_\infty(c)}{\varepsilon_0\varepsilon^0_{dc}}\tau_s. \tag{5}$$

The identity $\varepsilon_\infty(c) = \varepsilon_\infty(c = 0)$ is assumed in calculating (5). The kinetic depolarization mechanism adds to the decrements due to dilution of free and H-bonded water molecules and the internal depolarizing fields. Recently, terahertz time-domain spectroscopy data also confirmed that hydrodynamic motions of water molecules resulting from movement of ions contribute significantly to polarization deficiency.[38] At higher concentrations (above ~1 mol/l), the presence of a pronounced minimum and the subsequent increase of static permittivity have been observed by Sega *et al.*[39] through a non-equilibrium molecular dynamics simulation. Sega *et al.* proposed a phenomenological modification of the Hubbard–Onsager theory due to *screening effect*, which is physical intuited and suggests that the local field of the ions, which determines the torque on water molecules, should be screened by the presence of oppositely charged ions in its vicinity. They introduced a mean-field correction factor $\exp(-\kappa_0 c^{0.5} R)$ to (4), where κ_0 (m^{-1}) is defined in (6) and R (m) is the ionic radius, to take into account screening effects. In this paper, however, we tackle such non-idealities at higher concentrations through developing a model for ionic conductivity.

Considering a set of assumptions regarding the system of non-ideal electrolyte solutions, Debye, Huckel, and Onsager (DHO) derived a fundamental treatment to consider the total effects of non-ideality (friction, electrophoretic, and asymmetric relaxation effects) on the ionic conductivity. The complete derivation of DHO theory has been extensively discussed by Wright.[40] In order to calculate the specific conductivity of a general multivalent electrolyte system A_xB_y composed of A^{y+} and B^{x-} ion species with electron valency $z_1 = y$ and $z_2 = -x$ for cation and anion, respectively, and at temperature T in kelvin (K), we start our analysis by defining the concentration-independent inverse Debye length κ_0 (m^{-1}) as

$$\kappa_0 = \sqrt{\frac{e^2 N_A}{\varepsilon_0\varepsilon^0_{dc}k_BT}\left(|z_2|z_1^2 + |z_1|z_2^2\right)}, \tag{6}$$

where $e = 1.60 \times 10^{-19}$ C is the elementary charge, $N_A = 6.02 \times 10^{23}$ mol^{-1} is Avogadro's number, $\varepsilon_0 = 8.85 \times 10^{-12}$ F/m is the free space permittivity, and $k_B = 1.38 \times 10^{-23}$ J/K is the Boltzmann constant. After carefully performing a few mathematical steps, the electrophoretic coefficient, a ($m^{3.5}$ $S/mol^{1.5}$), and the asymmetric relaxation coefficient, b ($m^{3.5}$ $S/mol^{1.5}$), can be written as

$$a = |z_2|\frac{z_1^2 Fe\kappa_0}{6\pi\eta} + |z_1|\frac{z_2^2 Fe\kappa_0}{6\pi\eta} \tag{7}$$

$$b = |z_2|\frac{z_1^2 e^2\kappa_0}{24\pi\varepsilon_0\varepsilon^0_{dc}k_BT}\frac{1}{1+\sqrt{0.5}}\lambda_1 + |z_1|\frac{z_2^2 e^2\kappa_0}{24\pi\varepsilon_0\varepsilon^0_{dc}k_BT}\frac{1}{1+\sqrt{0.5}}\lambda_2, \tag{8}$$

where $F = 96\,485.33$ C/mol is the Faraday constant, η (kg m^{-1} s^{-1}) is the dynamic viscosity of the pure water, and λ_1 (m^2S/mol) and λ_2 (m^2S/mol) are the ionic conductivities of cation and anion, respectively, at infinite dilution. The infinite molar conductivity of the whole system at infinite dilution, Λ^∞ (m^2S/mol), is then

$$\Lambda^\infty = |z_2|\lambda_1 + |z_1|\lambda_2. \tag{9}$$

The molar conductivity of the whole system, $\Lambda(c)$ (m^2S/mol), can be calculated as a function of solute concentration c (mol/l) according to

$$\Lambda(c) = \Lambda^\infty - B\sqrt{10^3 c} \tag{10}$$

$$B = a + b, \tag{11}$$

where B is the coefficient combining the non-idealities of electrophoretic and relaxation effects. Finally, the specific conductivity $\sigma(c)$ (S/m) of the solution, calculated through theoretical formulations directly, can be expressed as

$$\sigma(c) = 10^3 c\Lambda(c). \tag{12}$$

In cases of low-concentration solutions for which concentration is of the order of mmol/l, it is more convenient to report the specific conductivity in μS/cm. Table II lists the input quantities required to

TABLE II. Input quantities required to model the specific conductivity and kinetic depolarization contribution to the static permittivity of NaCl, $NaNO_3$, and Na_2SO_4 at 25 °C according to (10) and (11). For NaCl and $NaNO_3$, $z_1 = 1$ and $z_2 = -1$, whereas for Na_2SO_4, $z_1 = 1$ and $z_2 = -2$. $\eta = 8.934 \times 10^{-4}$ (kg m^{-1} s^{-1}),[41] $\rho = 997.06$ (g/l).[41] Ionic conductivity values λ_1 and λ_2 are taken from Ref. 42. Debye–Falkenhagen (DF) coefficient D is calculated from (17) for each electrolyte system. The ionic radius of Na^+ = 102 (pm), Cl^- = 181 (pm), NO_3^- = 206 (pm), and SO_4^{2-} = 258 (pm) is also taken from Ref. 9.

Ion	M (g/mol)	λ_1 (m^2S/mol)	λ_2 (m^2S/mol)	Λ^∞ (m^2S/mol)	B ($m^{3.5}$S/$mol^{1.5}$)	D ($m^{1.5}$ $mol^{-0.5}$)
NaCl	58.4428	50.1×10^{-4}	76.4×10^{-4}	126.5×10^{-4}	2.83×10^{-4}	0.118
$NaNO_3$	84.9947	50.1×10^{-4}	71.4×10^{-4}	121.5×10^{-4}	2.79×10^{-4}	0.118
Na_2SO_4	142.0421	50.1×10^{-4}	160×10^{-4}	260.2×10^{-4}	19.2×10^{-4}	0.405

theoretically calculate the specific conductivity and kinetic depolarization contribution.

Note that the main purpose of exploiting DHO theory to calculate the conductivity, rather than using the measured conductivity directly, is to build an analytical model for kinetic depolarization mechanism, which will eventually be incorporated into a semi-empirical static permittivity model. Such an approach helps to develop a model that is as independent as possible from external measured parameters. For the range of ion concentrations of the present work (~mmol/l), the value of conductivities calculated analytically through DHO theory and the measured ones are in good agreement with each other and with the literature.[43–45]

C. Dielectric saturation

Around the solvation layers of an ion, the rotational ability of the electric dipole moment of solven molecules appears to be reduced by proximity to the associated Columbic field. If the ion–solvent interactions of water molecules located in the hydration layers of an ion are much stronger than the interactions to outer H-bonded water molecules, the water molecules in the hydration layers effectively become immobilized and may not be affected by the presence of an external applied field. A resulting polarization deficiency, known as dielectric saturation, can be evaluated in terms of the number of irrotational bonded (IB) water molecules $Z^{+}{}_{IB}$ and $Z^{-}{}_{IB}$ per cation and anion, respectively. For a general multivalent electrolyte system A_xB_y, the water molecules adjacent to cation and anion, numbered $Z_{IB} = xZ^{+}{}_{IB} + yZ^{-}{}_{IB}$, do not contribute to the static permittivity. The Z_{IB} values of monovalent ions reported in the literature[22] indicate that cations, which have smaller ionic radius than anions relatively, are more extensively surrounded by water molecules than anions, with the number of water molecules in the solvation layers decreasing with increasing ionic radius.[35] In addition, more highly charged cations and anions (multivalent ions) have greater Z_{IB} values than monovalent ions, suggesting the existence of irrotationally bound water molecules beyond the first solvation layer. Recent computer simulations[46,47] and dielectric spectroscopy studies[22] of aqueous solutions also concluded that the ions influence the water molecules in the first hydration layer as well as the H-bonded water molecules nearby. Noting that effects of ionic radius, electron valency, and long-range interactions are not accounted for in the mixture relation (3), the contribution of dielectric saturation to a semi-empirical model describing static permittivity must be added separately. Although there have been yet no theoretical approaches to directly calculate Z_{IB} from the characteristics of solute particles, a comparison of the apparent solvent concentration $c_s^{ap}(c)$ calculated from measured $\varepsilon_{dc}(c)$, with the analytical solvent concentration $c_s^0 = \rho_{\text{water}}/M_{\text{water}}$ at zero solute concentration, leads to the calculation of $Z_{IB}(c)$ as[14]

$$Z_{IB}(c) = \frac{c_s^0 - c_s^{ap}(c)}{c}. \tag{13}$$

In order to compare Z_{IB} values of the present samples in this work with the literature values presented in Sec. IV, scaled Cavell equation[14,48] is used for the calculation of $c_s^{ap}(c)$ as follows:

$$c_s^{ap}(c) = F_{Cav}^0 \frac{2\bar{\varepsilon}_{dc}(c) + 1}{\bar{\varepsilon}_{dc}(c)} [\bar{\varepsilon}_{dc}(c) - \varepsilon_\infty(c)] \tag{14}$$

$$F_{Cav}^0 = c_s^0 \frac{\varepsilon_{dc}^0}{\left(2\varepsilon_{dc}^0 + 1\right)\left(\varepsilon_{dc}^0 - \varepsilon_\infty^0\right)}, \tag{15}$$

where $\bar{\varepsilon}_{dc}(c) = \varepsilon_{dc}(c) + \delta_{KD}(c)$ is the static permittivity corrected for kinetic depolarization to prevent unreasonably large values of Z_{IB} for almost all electrolyte systems.[49] $\bar{\varepsilon}_{dc}(c)$, thus, is taking into account solvent-affiliated contributions due to dilution and internal depolarizing field as well as dielectric saturation. The field factor $f_i(c) = f_i(0)$ and $A_i = 1/3$ for spherical reaction field are assumed in the original equation.[14] Several other approaches including Kirkwood–Frohlich (KF) equation[11] and Bruggeman relation[10] have also been employed for the calculation of $c_s^{ap}(c)$. A direct comparison of Z_{IB} values from different models, however, requires careful attention since for a given electrolyte system the Z_{IB} value becomes model dependent[13] and thus no particular model is yet preferred. In order to form a semi-empirical model of the static permittivity with no *a priori* information of Z_{IB} values for the calculation of polarization deficiency due to dielectric saturation mechanism $\delta_{sat}(c)$, we treat it as a linear function of solute concentration,

$$\delta_{sat}(c) = \gamma_{sat} c, \tag{16}$$

where γ_{sat} is an adjustable parameter obtained through a data-fitting procedure, for each electrolyte system.

D. Ionic atmosphere polarization

The concept of ionic atmosphere, as first dealt by the model presented by Debye and Huckel in 1927 for the conductivity of strong electrolyte systems, can be defined in terms of a chosen reference ion, with all the other ions including cations and anions distributed around it, making up the ionic atmosphere. In the absence of the external electric field, the ionic atmosphere is symmetric with the charge distribution tending to zero with distance from the reference ion.[40] If the reference ion is a cation moving under the influence of an external electric field, however, it and the cations of the ionic atmosphere will move in the direction of the applied field, while the anions will move in the opposite direction. This movement therefore causes a deficit of negative charges in front of the moving reference cation and an excess of negative charge behind it, causing asymmetry in the ionic atmosphere around the moving reference ion. Under alternating electric field, the development of the asymmetric ionic atmosphere depends on the frequency, in particular on whether there is enough time available to reach the asymmetric state. The frequency-dependent asymmetric ionic atmosphere, as first theoretically predicted by Debye and Falkenhagen,[24,50] introduces additional polarization of quasi-elastic origin to the system, without any dipolar species resulting from ion association and chemical reaction [different from ion-pairs (IP)]. The Debye–Falkenhagen (DF) effect suggests a rise in static permittivity above that of pure water at very low concentrations. For a typical ~10 mmol/l solution of a 1:1 electrolyte system, the relaxation of the asymmetric ionic atmosphere is predicted to occur below 100 MHz.[51,52] The DF effect is, alternatively, recognized as increasing ionic conductivity at around the frequency corresponding to the relaxation of the asymmetric ionic atmosphere.[52,53] Articles published prior to this work do not unambiguously establish any positive contribution of the DF effect to static permittivity. This is mainly because, as frequency decreases, the loss tangent ($\propto \sigma/2\pi f\varepsilon_0$) is so great and the electrode polarization

effects so marked that the required accuracy is not available.[54] In such cases, it would not be feasible to employ a double-term Debye model to account for contributions of low-frequency asymmetric ionic atmosphere (DF relaxation) and high-frequency hydrogen-bond water relaxation. There is, however, a possibility that part of the DF type relaxation trace could be captured at higher frequencies than its relaxation frequency. Prior dilute solution measurements have shown the static permittivity to be smaller than that of pure water[55,56], and some have shown the opposite. Van Beek and Mandel[51] were first to experimentally report the increment in static permittivity. For most aqueous solutions investigated in their work, including alkali chlorides in water, static permittivity shows an initial increase above the value of the pure solvent with the values up to concentrations of 25 mmol/l. Further initial evidence of the existence of DF effect in NaCl aqueous solutions was implicitly mentioned by Winsor and Cole[57] and Nörtemann *et al.*[10]

The static permittivity increment based on speculative theoretical estimation by Debye and Falkenhagen, which is equal to D multiplied by $(10^3 c)^{0.5}$, where D ($m^{1.5}$ $mol^{-0.5}$) is the Debye–Falkenhagen (DF) coefficient[50,51] as

$$D = \frac{|z_1 z_2| e^2 \kappa_0 q^{1.5}}{24\pi\varepsilon_0 k_B T (1 + q^{0.5})^2}, \tag{17}$$

where κ_0 (m^{-1}) is given in (6) and q is

$$q = \frac{|z_1 z_2|(\lambda_1 + \lambda_2)}{(|z_1| + |z_2|)(|z_1|\lambda_2 + |z_2|\lambda_1)}, \tag{18}$$

gives relatively larger effects at low concentrations.[57] As a result, we add an adjustable parameter γ_{DF_1} to correct for DF coefficient during the fitting procedure. Moreover, as the DF effect was originally derived for dilute concentrations and will be amplified as concentration increases, a decaying factor $\Gamma(c)$ should be introduced to correct for the theoretical expression as concentration increases.[51] The decaying function, as will be shown in Sec. IV, is also needed to obtain reasonable values for irrotational bonded (IB) water molecules Z_{IB}. In this work, an exponential-type decaying function $\Gamma(c)$, inspired by the concept of *screening* factor,[39] which includes contributions from induced dipolar moment length (concentration-independent Debye length) $1/\kappa_0$ and ionic radius of cation R^+ and anion R^-, is established. An adjustable parameter γ_{DF_2} is also added to provide a higher quality of fit between the measured data and the proposed model of the static permittivity in the given concentration range. The net static permittivity increment due to the DF effect $\delta_{DF}(c)$ can then be written as

$$\delta_{DF}(c) = \gamma_{DF_1} D\sqrt{10^3 c}\,\Gamma(c) \tag{19}$$

$$\Gamma(c) = \exp\left[-\gamma_{DF_2}\kappa_0\left(\frac{R^+ + R^-}{2}\right)c^{0.5}\right], \tag{20}$$

where κ_0 is calculated through (6) and the values of ionic radius, R^+ and R^-, for Na^+, Cl^-, NO_3^-, and SO_4^{2-} are listed in Table II. More discussion on the effects of concentration-independent Debye length $1/\kappa_0$ and effective ionic radius R on the Debye–Falkenhagen effect will be addressed in Sec. IV C.

E. Complete model of static permittivity

According to the discussions made through Subsections III A–III D, the semi-empirical model to represent the static permittivity of multivalent electrolyte systems in low-concentration regime can be given as a combination of terms from (3), (4), (16), and (19)

$$\begin{aligned}\varepsilon_{dc}(c) &= \varepsilon_{dc}^0 + \delta_{DF}(c) - \delta_{MW}(c) - \delta_{KD}(c) - \delta_{sat}(c)\\ &= \varepsilon_{dc}^0 + \gamma_{DF_1} D\sqrt{10^3 c}\exp\left[-\gamma_{DF_2}\kappa_0\left(\frac{R^+ + R^-}{2}\right)c^{0.5}\right]\\ &\quad - \delta_{MW}(c) - \delta_{KD}(c) - \gamma_{sat} c,\end{aligned} \tag{21}$$

where $\delta_{MW}(c)$ and $\delta_{KD}(c)$ are directly calculated through (3)–(12), D is calculated from (17) and is given in Table II, and $\delta_{DF}(c)$ along with $\delta_{sat}(c)$ is calculated empirically through the adjustable parameters γ_{DF_1}, γ_{DF_2}, and γ_{sat} by careful execution of the data-fitting procedure. The effects discussed in Subsections III A–III D have each been treated separately, effectively ignoring possible interrelations between each other. Thus, comparison with experimental results needs stringent attention. It is also worth mentioning that in highly concentrated solutions, the ionic contributions, based on Bjerrum's concept of ion-pairs, generally increase. In the case of highly concentrated solutions, it may be necessary to add the incremental effect of ion-pairs (IP) $\delta_{IP}(c)$ to the model of static permittivity represented in (21). Analysis of dielectric spectra proves to be more complicated, but manageable, if ion-pairs and complex aggregates also contribute to the complex permittivity.[58] For example, a composite of ion-cloud and ion-pair relaxations is manifested through a small relaxation peak at lower frequencies in NaCl aqueous solutions for concentrations above 1 mol/l.[59] In the concentration ranges for the electrolyte systems studied in this work, however, no evidence of creation of strong ion-pairs has been observed.

IV. RESULTS AND DISCUSSION

The extracted Debye relaxation parameters, i.e., ε_{dc}, ε_∞, τ, and σ, along with the associated uncertainties for each of NaCl, $NaNO_3$, and Na_2SO_4 electrolyte systems at $T = 25\,^\circ C$ are listed in previous work.[16] The major relaxation of the spectra for NaCl, $NaNO_3$, and Na_2SO_4 electrolyte systems occurs at around 18 GHz at $T = 25\,^\circ C$, corresponding to cooperative relaxation of the H-bond network of bulk water molecules, as shown in Fig. 1. The minor high-frequency relaxation process (~120 GHz), which is due to free water molecules, is beyond the upper frequency limit of the measurement apparatus used in the present work. Static permittivity, ε_{dc}, is plotted vs concentration in Fig. 2, with semi-empirical models that are described in the following paragraph.

A. Evaluation of semi-empirical model

Here, the semi-empirical model developed for static permittivity is evaluated and the contributions of different mechanisms presented in Sec. III are discussed. In Fig. 2, the static permittivity for aqueous solutions of NaCl, $NaNO_3$, and Na_2SO_4 is plotted vs concentration. The fitted static permittivity modeled by (21) is also shown for each electrolyte system, with parameters given in Table III. The permittivity of NaCl,[10–12] $NaNO_3$,[8,9] Na_2SO_4[13,14]

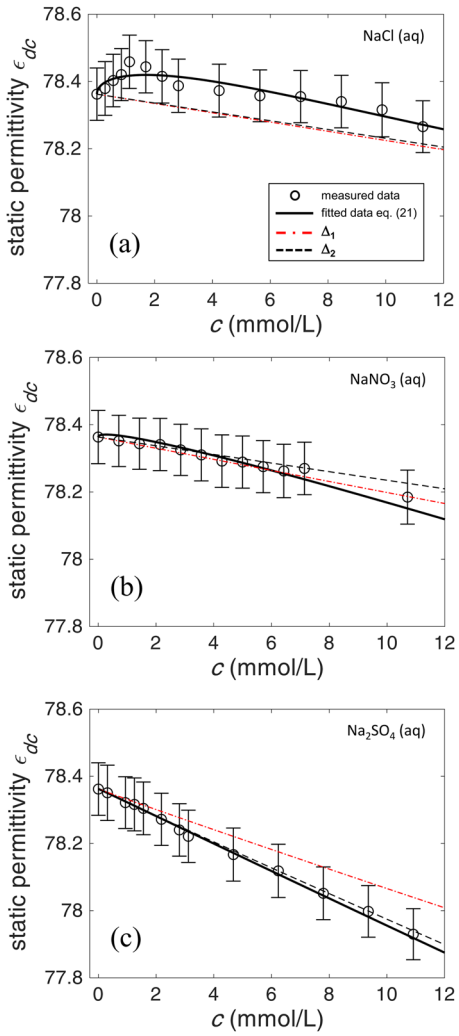

FIG. 2. Experimental data (open circles) of the static permittivity, ε_{dc}, and fitted semi-empirical model of static permittivity (21) (solid line) with parameters listed in Table III of aqueous solutions of (a) NaCl, (b) $NaNO_3$, and (c) Na_2SO_4 at $T = 25\,^{\circ}C$. The decrement term Δ_1 (22) accounts for the contributions of dilution and kinetic depolarization (dashed-dotted line), and Δ_2 (23) accounts for the contributions of dilution, kinetic depolarization, and dielectric saturation, where Z_{IB} values are taken from the literature[22] and are treated as input variables (dashed line). The static permittivity data ε_{dc} are obtained from Ref. 16.

and indeed most other strong electrolytes in water has already been found to follow a decreasing trend with concentration for $c \approx 0.5$ mol/l–5 mol/l (500 mmol/l–5000 mmol/l). Within the concentration range of the present work, however, the static permittivities so obtained show a slight increase with concentration for both NaCl and $NaNO_3$, while they show almost linear decrease for Na_2SO_4. The positive contribution to static permittivity in this low-concentration regime can be best attributed to the creation of ionic atmosphere polarization and the associated Debye–Falkenhagen (DF) effect, as discussed in Sec. III. Neglecting the DF effect, i.e., $\delta_{DF} = 0$ in (21), to fit the measured static permittivity values ε_{dc} within the uncertainty limits $u(\varepsilon_{dc})$ will deteriorate the fitting through least-squares analysis. Moreover, it would not be conceivable to explain the overestimated values of measured ε_{dc} values (even on the lower bound of the error bars), which lead to unrealistic negative values of irrotationally bound water molecules Z_{IB} (discussed in Sec. IV B). The contribution of the DF effect to the static permittivity represented by γ_{DF_1} (or $\gamma_{DF_1} D$) behaves as $\gamma_{DF_1}(\mathrm{NaCl}) > \gamma_{DF_1}(\mathrm{NaNO_3}) > \gamma_{DF_1}(\mathrm{Na_2SO_4})$. The permittivity increment for NaCl is in conformity with the findings of van Beek and Mandel[51] and Winsor and Cole,[57] although Anderson[54] commented on the possible challenges that might in general question the observation of DF effect through experiments. Static permittivity data in low-concentration regions, which can potentially manifest the DF effect in $NaNO_3$ and Na_2SO_4, however, have not been yet reported in the literature.

The resulting decrements in measured static permittivity of all electrolyte systems shown in Fig. 2 with concentration (albeit with an initial increase for NaCl and $NaNO_3$, which will be discussed in Subsection IV C) can be attributed to the sum of contributions from dilution and internal depolarizing field, kinetic depolarization, and dielectric saturation, as well as the vanishing effect of DF effect through $\exp[-\gamma_{DF_2}\kappa_0((R^+ + R^-)/2)c^{0.5}]$. The dielectric saturation effect, represented by γ_{sat}, follows the trend $\gamma_{sat}(\mathrm{Na_2SO_4}) > \gamma_{sat}(\mathrm{NaNO_3}) > \gamma_{sat}(\mathrm{NaCl})$. In principle, such a sequence is connected to an increase in the number of irrotationally bound water molecules Z_{IB} within the concentration range studied.

Two decrement terms of static permittivity, Δ_1 and Δ_2, which are calculated according to

$$\Delta_1 = \varepsilon_{dc}^0 - [\delta_{MW}(c) + \delta_{KD}(c)] \tag{22}$$

and

$$\Delta_2 = \varepsilon_{dc}^0 - [\delta_{MW}(c) + \delta_{KD}(c) + \delta_{sat}(c)], \tag{23}$$

TABLE III. Concentration, ε_{dc}^0, and parameters of semi-empirical static permittivity model (21) of aqueous NaCl, $NaNO_3$, and Na_2SO_4 solutions at 25 °C. The sum of squared error (SSE) for each fitted curve is also shown.

	c (mmol/l)	ε_{dc}^0	γ_{DF_1} ($l^{0.5}/m^{1.5}$)	γ_{DF_2} (l/mol)	γ_{sat} (l/mol)	SSE
NaCl	0–11.28	78.362	0.98 ± 0.17	$1.04 \pm 0.42\times10^3$	0.74 ± 0.71	0.005
$NaNO_3$	0–17.85	78.358	0.28 ± 0.14	0.11 ± 0.03	13.7 ± 5.9	0.005
Na_2SO_4	0–12.47	78.362	0.015 ± 0.005	0.054 ± 0.018	14.9 ± 5.3	0.002

are also shown in Fig. 2 for each electrolyte system. Therein, ε_{dc}^{0} is the static permittivity of deionized water,[16] and $\delta_{MW}(c)$ and $\delta_{KD}(c)$ are calculated from (3) and (4), respectively. The calculation of $\delta_{sat}(c)$, i.e., $\delta_{sat}(c) = \varepsilon_{dc}^{0} - \bar{\varepsilon}_{dc}(c) - \delta_{MW}(c)$, where $\bar{\varepsilon}_{dc}(c)$ is implicitly calculated from (14), requires input values for Z_{IB}. The Z_{IB} values are measurable only for the whole system A_XB_Y, so it is necessary to split them into the ionic $Z^{+}{}_{IB}$ and $Z^{-}{}_{IB}$ values. Cationic irrotationally bound water molecules have $Z^{+}{}_{IB} = 4.2$ for Na^{+},[11] and anionic irrotationally bound water molecules have $Z^{-}{}_{IB} = 0$ for Cl^{-},[11] 0 for NO_3^{-},[22] and 10 for SO_4^{2-}.[14] These numbers, however, are obtained from experimental data for electrolyte systems with moderate to high concentrations, i.e., 0.5 mol/l < c < 5 mol/l. The decrement term Δ_1 accounts for the reduction of static permittivity due to dilution and internal depolarizing field, and kinetic depolarization, while Δ_2 accounts for contributions of the same mechanisms as well as dielectric saturation.

Ideally, one would expect $\Delta_2 < \Delta_1$ as the sum of contributions from dilution and internal depolarizing field, kinetic depolarization, and dielectric saturation would be greater than the sum of the first two. This, however, is not held for the corresponding calculated results for NaCl and $NaNO_3$ [Figs. 2(a) and 2(b)] within the low-concentration range as $\Delta_2 > \Delta_1$. The authors' calculations already showed that there are higher concentrations $c > 200$ mmol/l for NaCl (aq) and $c > 500$ mmol/l for $NaNO_3$(aq), where $\Delta_2 < \Delta_1$ is satisfied with the reported literature values for irrotationally bound water molecules Z_{IB}.[9,11,22] This observation reflects that there are unrealistic negative values for dielectric saturation $\delta_{sat}(c)$, which are calculated from Z_{IB} values taken from the literature. Therefore, it can be inferred that the number of irrotationally bound water molecules Z_{IB} reported in the literature for either cation Na^{+} or anions Cl^{-} and NO_3^{-} is underestimated in the low-concentration regime. For Na_2SO_4 [Fig. 2(c)], however, as $\Delta_2 < \Delta_1$ holds, the same, at least comparable, number of Z_{IB} for cation Na^{+} and anion SO_4^{2-} is speculated.

B. Irrotationally bound water molecules Z_{IB}

The number of irrotationally bound water molecules Z_{IB} for each electrolyte solution can be calculated as a function of concentration, through (13)–(15). A calculation of the Z_{IB} values from (14) using $\bar{\varepsilon}_{dc}$, the static permittivity corrected for kinetic depolarization, has given unrealistic negative values for NaCl and $NaNO_3$, as depicted in Fig. 3. The topic of underestimated Z_{IB} values was also discussed by Wachter *et al.*[9] for various salts including $NaNO_3$. They concluded that the possible presence of an additional low-frequency relaxation "not due to water" was the only plausible explanation for the observed anomalous values of Z_{IB}. Buchner *et al.*[11] also rejected the Z_{IB} values obtained at lower concentrations (c < 1 mol/l) as the measurement uncertainty was too large to yield reliable information from their extrapolated data at that concentration range. These unrealistic values offer support for the veracity of the observed positive contribution of ionic atmosphere and DF effect to the static permittivities at low concentrations. Attempting to obtain realistic non-negative values for Z_{IB} can be achieved by correcting $\bar{\varepsilon}_{dc}$ values in (14) for DF effect, i.e., $\bar{\varepsilon}_{dc}(c) = \varepsilon_{dc}(c) + \delta_{KD}(c) - \delta_{DF}(c)$, where $\delta_{DF}(c)$ is calculated from (19) and (20) and the parameters obtained in Table III. The Z_{IB} values corrected for DF effect are also shown in Fig. 3.

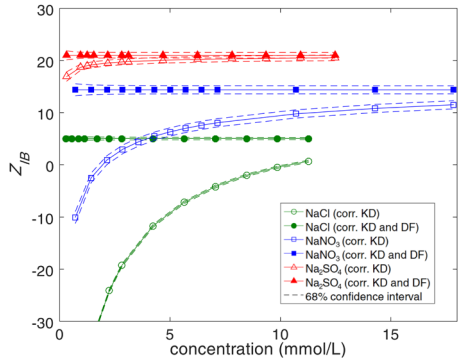

FIG. 3. Number of irrotationally bound water molecules, Z_{IB}, of NaCl (circle), $NaNO_3$ (square), and Na_2SO_4 (triangle) at 25 °C. Z_{IB} values are corrected for kinetic depolarization (hollow symbols), and corrected for kinetic depolarization and Debye–Falkenhagen effect (filled symbols). 68% confidence intervals, representing the uncertainties in deriving Z_{IB} values, are also shown (dashed line). Fitted static permittivities (21) are used to calculate Z_{IB} through (13)–(15).

From the extrapolations of Z_{IB} at $c \to 0$, and by setting $Z^{+}{}_{IB} = 4.5 \pm 0.3$ for Na^{+},[11] $Z^{-}{}_{IB}$ values for each electrolyte solution are listed in Table IV. According to Table IV, $Z^{-}{}_{IB}$ values corrected only for kinetic depolarization ($Z^{-}{}_{IB}{}^{KD}$) result in negative values for NaCl and $NaNO_3$ solutions. The $Z^{-}{}_{IB}$ values, corrected for both kinetic depolarization and DF effect ($Z^{-}{}_{IB}{}^{KD+DF}$), however, result in non-negative and physically realistic values. These values read as 0.5 ± 0.6 for Cl^{-} and 11.9 ± 0.9 for SO_4^{2-} and are found to be in a good agreement with 0 ± 0.3 for Cl^{-} reported in Ref. 11 and 10 ± 0.7 for SO_4^{2-} reported in Ref. 14. Higher values, however, are calculated for NO_3^{-} as 9.9 ± 1.2 compared to 0 reported in Ref. 22. Although $Z^{-}{}_{IB}$ is not strictly a coordination number (CN) (total number of water molecules in all solvation layers of ion),[7] the level of agreement between coordination number of NO_3^{-}, i.e., 5.9–9,[9,22] and number of irrotationally bound water molecules around NO_3^{-}, i.e., 9.9 ± 1.2 (Table IV), largely reflects the presence of water molecules with reduced but non-zero rotational mobility in the structural mismatch region. As pointed out by Frank and Wen[28,61], there must exist a

TABLE IV. Number of irrotationally bound water molecules per anion, $Z^{-}{}_{IB}$, corrected for kinetic depolarization ($Z^{-}{}_{IB}{}^{KD}$), and corrected for kinetic depolarization and Debye–Falkenhagen effect ($Z^{-}{}_{IB}{}^{KD+DF}$). Fitted static permittivities (21) are used to calculate Z_{IB} through (13)–(15). $Z^{+}{}_{IB} = 4.2 \pm 0.3$ for Na^{+}[11] is assumed for all calculations. The coordination number (CN) and $Z^{-}{}_{IB}$ for each anion according to corresponding reference are also given.

	CN (ref)	$Z^{-}{}_{IB}$ (ref)[a]	$Z^{-}{}_{IB}{}^{KD}$	$Z^{-}{}_{IB}{}^{KD+DF}$
Cl^{-}	6[22,60]	0 ± 0.3[11]	−99.6 ± 0.6	0.5 ± 0.6
NO_3^{-}	5.9–9[9,22]	0[22]	−14.5 ± 1.2	9.9 ± 1.2
SO_4^{2-}	7–12[14,22]	10 ± 0.7[14]	7.9 ± 1.0	11.9 ± 0.9

[a] $Z^{-}{}_{IB}$ values are corrected for kinetic depolarization under slip boundary condition ($p = 2/3$).

structural mismatch region of water molecules with reduced but non-zero rotational mobility beyond the inner (first) solvation layer. At low concentration of NO_3^- ions (mmol/l), the number of water molecules is way greater than the number of ions ($c_s^0/c \sim 1000$); thus, those water molecules that could not find an ion to partner with in the inner solvation layer remain in the structural mismatch region. Water molecules with reduced but non-zero rotational mobility in the structural mismatch region, therefore, lead to an increase in the Z^-_{IB} value of NO_3^- ion.

Comparing the coordination number of SO_4^{2-}, i.e., 7–12,[14,22] and the number of irrotationally bound water molecules around SO_4^{2-}, i.e., 11.9 ± 0.9, implies that in the strong Coulombic field of bivalent ions, more water molecules are irrotationally bound in the first and beyond the first solvation layer.[14] Based on the coordination number of Cl^-, i.e., 6,[22,60] with a broad distribution from 1 to 8,[11] and the number of irrotationally bound water molecules around Cl^-, i.e., 0.5 ± 0.6, however, no water molecule is found to be bonded beyond the first solvation layer. Indeed, $Z^-_{IB} \neq 0$ offers a fraction number of water molecules in the first solvation layer that are immobilized within the low-concentration range studied. The uncertainty associated with the Z^-_{IB} value, however, may not allow one to derive a firm conclusion.

C. Debye–Falkenhagen effect

The analysis of DF effect for different electrolyte systems has not been extensively covered in the literature. Nevertheless, concentration-independent Debye length l_{κ_0} (m) is an available parameter that can be employed to justify the strength of DF effect for different ions. l_{κ_0} is calculated as[62]

$$l_{\kappa_0} = \frac{1}{\kappa_0}, \tag{24}$$

where κ_0 is the concentration-independent inverse Debye length calculated from (6). For NaCl and $NaNO_3$ which both have same ionic electron valency $z_1 = 1$, $z_2 = 1$, $l_{\kappa_0} = 9.60$ nm, and for Na_2SO_4 with $z_1 = 1$, $z_2 = 2$, $l_{\kappa_0} = 6.07$ nm at $T = 25\,^\circ$C. The Debye length, l_{κ_0}, can be taken as the corresponding length of the induced dipolar moment created by charge cloud separation of ionic atmosphere. Therefore, the longer the Debye length, the stronger is the induced dipolar moment and thereby the DF effect. As NaCl and $NaNO_3$ possess longer Debye length than Na_2SO_4, according to γ_{DF_1} listed in Table III, the positive contribution of DF effect follows expectedly the trend $\varepsilon_{dc}(NaCl) > \varepsilon_{dc}(Na_2SO_4)$ and $\varepsilon_{dc}(NaNO_3) > \varepsilon_{dc}(Na_2SO_4)$.

The strength of DF effect, however, should not be solely dependent on Debye length as we should be able to justify the difference in DF effect of $\varepsilon_{dc}(NaCl) > \varepsilon_{dc}(NaNO_3)$ with the same Debye length. A potential hypothesis can be attributed to "electrophoretic effect"[40] that prevents the formation of complete asymmetric ionic atmosphere. While the asymmetric ionic atmosphere is forming under the applied electric field, the ions with opposite charges are passing each other. As water molecules (in solvation layers) are pulled along with each ion, each ion (cation and anion), in effect, will see water molecules streaming past itself in the opposite direction, and this will exert a viscous drag on each ion, slowing it down to form a complete (longer) asymmetric ionic atmosphere. As the coordination number $CN(Cl^-) < CN(NO_3^-)$ (Table IV) which is also proportional to ionic radius $R\,(Cl^-) < R\,(NO_3^-)$ (Table II), and according to the electrophoretic effect, there are less water molecules to create viscous drags in the ionic atmosphere of Na^+ and Cl^-; thus, a longer asymmetric ionic atmosphere will be formed. As a result, the positive contribution of DF effect will follow the trend $\varepsilon_{dc}(NaCl) > \varepsilon_{dc}(NaNO_3)$.

V. CONCLUSION

The dielectric properties of environmentally relevant low-concentration electrolyte solutions of NaCl, $NaNO_3$, and Na_2SO_4, which are commonly found in water sources, have been analyzed through well-controlled laboratory experiments. A semi-empirical parametric model to represent the static permittivity has been represented. The model has efficiently accounted for contributions due to dilution and internal depolarizing fields, kinetic depolarization, dielectric saturation, and the Debye–Falkenhagen effect. The results have shown that the decrements in static permittivity due to aggregation of dilution and internal depolarizing field, kinetic depolarization, and dielectric saturation follow the trend $\varepsilon_{dc}(Na_2SO_4) < \varepsilon_{dc}(NaNO_3) < \varepsilon_{dc}(NaCl)$. It has also been demonstrated that, within the low-concentration range studied, the static permittivities need to be corrected to incorporate the contributions of both kinetic depolarization and Debye–Falkenhagen effect, to obtain a non-negative and physically realistic number of irrotationally bound water molecules per anion. Rather, a large number of irrotationally bound water molecules for $NaNO_3$, however, suggests the existence of a structural mismatch region of water molecules with reduced but non-zero rotational mobility that do not contribute to polarization. Moreover, it has been observed that in NaCl and $NaNO_3$ solutions, there is significant positive contribution due to the Debye–Falkenhagen effect that increases the static permittivity, particularly at lower concentrations. The concentration-independent Debye screening length has been defined to justify the strength of the DF effect for the electrolyte solutions studied. This parameter has also been discussed to be possibly related to the electrophoretic effect and the coordination number, leading to the DF effect strength to be greater for NaCl compared to $NaNO_3$ and Na_2SO_4.

Further measurements and highly accurate experimental data for different electrolyte solutions at various temperatures are desirable to evaluate the semi-empirical parametric model, examine the number of irrotationally bound water molecules, and also extend our knowledge of ionic atmosphere polarization and positive contribution of the DF effect to static permittivities in low-concentration regions. Studying the cluster of water molecules that are hydrating the Cl^-, NO_3^-, and SO_4^{2-} ions will also be of great interest in understanding the coordination number and ionic atmosphere under an applied electric field.

ACKNOWLEDGMENTS

This work was funded by the USDA-National Institute of Food & Agriculture, Award No. 013025-00001. The authors gratefully acknowledge Amy L. Kaleita for her leadership on this project.

DATA AVAILABILITY

The data that support the findings of this study are available at https://doi.org/10.1088/1361-6501/aac8c2, reference number [16].

REFERENCES

[1] B. A. Zimmerman and A. L. Kaleita, "Dissolved constituents in agricultural drainage waters," Trans. ASABE **60**, 847–859 (2017).

[2] R. Buchner, "What can be learnt from dielectric relaxation spectroscopy about ion solvation and association?," Pure Appl. Chem. **80**, 1239–1252 (2008).

[3] U. Kaatze, "Complex permittivity of water as a function of frequency and temperature," J. Chem. Eng. Data **34**, 371–374 (1989).

[4] N. Vinh, M. S. Sherwin, S. J. Allen, D. George, A. Rahmani, and K. W. Plaxco, "High-precision gigahertz-to-terahertz spectroscopy of aqueous salt solutions as a probe of the femtosecond-to-picosecond dynamics of liquid water," J. Chem. Phys. **142**, 164502 (2015).

[5] U. Kaatze, V. Lönnecke, and R. Pottel, "Dielectric spectroscopy of aqueous $ZnCl_2$ solutions. Dependence upon solute concentration and comparison with other electrolytes," J. Mol. Liq. **34**, 241–255 (1987).

[6] A. Lyashchenko and A. Y. Zasetsky, "Complex dielectric permittivity and relaxation parameters of concentrated aqueous electrolyte solutions in millimeter and centimeter wavelength ranges," J. Mol. Liq. **77**, 61–75 (1998).

[7] W. Wachter, Š. Fernandez, R. Buchner, and G. Hefter, "Ion association and hydration in aqueous solutions of LiCl and Li_2SO_4 by dielectric spectroscopy," J. Phys. Chem. B **111**, 9010–9017 (2007).

[8] A. Lileev, Z. Filimonova, and A. Lyashchenko, "Dielectric permittivity and relaxation in aqueous solutions of alkali metal sulfates and nitrates in the temperature range 288–313 K," J. Mol. Liq. **103-104**, 299–308 (2003).

[9] W. Wachter, W. Kunz, R. Buchner, and G. Hefter, "Is there an anionic Hofmeister effect on water dynamics? Dielectric spectroscopy of aqueous solutions of NaBr, NaI, $NaNO_3$, $NaClO_4$, and NaSCN," J. Phys. Chem. A **109**, 8675–8683 (2005).

[10] K. Nörtemann, J. Hilland, and U. Kaatze, "Dielectric properties of aqueous NaCl solutions at microwave frequencies," J. Phys. Chem. A **101**, 6864–6869 (1997).

[11] R. Buchner, G. T. Hefter, and P. M. May, "Dielectric relaxation of aqueous NaCl solutions," J. Phys. Chem. A **103**, 1–9 (1999).

[12] E. Levy, A. Puzenko, U. Kaatze, P. B. Ishai, and Y. Feldman, "Dielectric spectra broadening as the signature of dipole-matrix interaction. I. Water in nonionic solutions," J. Chem. Phys. **136**, 114502 (2012).

[13] J. Barthel, H. Hetzenauer, and R. Buchner, "Dielectric relaxation of aqueous electrolyte solutions II. Ion-pair relaxation of 1:2, 2:1, and 2:2 electrolytes," Ber. Bunsengesellschaft Phys. Chem. **96**, 1424–1432 (1992).

[14] R. Buchner, S. G. Capewell, G. Hefter, and P. M. May, "Ion-pair and solvent relaxation processes in aqueous Na_2SO_4 solutions," J. Phys. Chem. B **103**, 1185–1192 (1999).

[15] A. Gorji, A. L. Kaleita, and N. Bowler, "Towards low-cost sensors for real-time monitoring of contaminant ions in water sources," in *Microwave Symposium (IMS), 2017 IEEE MTT-S International, Honolulu, HI, USA* (IEEE, 2017), pp. 1–4.

[16] A. Gorji and N. Bowler, "Dielectric measurement of low-concentration aqueous solutions: Assessment of uncertainty and ion-specific responses," Meas. Sci. Technol. **29**, 085801 (2018).

[17] H. Weingärtner, A. Knocks, W. Schrader, and U. Kaatze, "Dielectric spectroscopy of the room temperature molten salt ethylammonium nitrate," J. Phys. Chem. A **105**, 8646–8650 (2001).

[18] T. Fukasawa, T. Sato, J. Watanabe, Y. Hama, W. Kunz, and R. Buchner, "Relation between dielectric and low-frequency Raman spectra of hydrogen-bond liquids," Phys. Rev. Lett. **95**, 197802 (2005).

[19] P. R. Bevington and D. K. Robinson, in *Data reduction and error analysis for the physical sciences* (McGraw-Hill, 2010), Chap. 8.

[20] I. BIPM, I. IFCC, I. IUPAC, and O. ISO, "Evaluation of measurement data—Guide for the expression of uncertainty in measurement," International Organization for Standardization JCGM 100 (2008).

[21] A. Gregory, R. Clarke, and M. Cox, "Traceable measurement of dielectric reference liquids over the temperature interval 10–50 °C using coaxial-line methods," Meas. Sci. Technol. **20**, 075106 (2009).

[22] R. Buchner and G. Hefter, "Interactions and dynamics in electrolyte solutions by dielectric spectroscopy," Phys. Chem. Chem. Phys. **11**, 8984–8999 (2009).

[23] R. Buchner, J. Barthel, and J. Stauber, "The dielectric relaxation of water between 0 °C and 35 °C," Chem. Phys. Lett. **306**, 57–63 (1999).

[24] H. Falkenhagen and W. Fischer, "Dependence of electrical conductance and dielectric constant upon frequency in mixtures of strong electrolytes," Nature **130**, 928 (1932).

[25] J. C. Lestrade, J. P. Badiali, and H. Cachet, "Dielectric relaxation processes in electrolyte solutions," in *Dielectric and Related Molecular Processes*, edited by M. Davies (The Royal Society of Chemistry, 1975), Vol. 2, pp. 106–150.

[26] U. Kaatze, R. Behrends, and R. Pottel, "Hydrogen network fluctuations and dielectric spectrometry of liquids," J. Non-Cryst. Solids **305**, 19–28 (2002).

[27] H. L. Friedman, C. Krishnan, and C. Jolicoeur, "Ionic interactions in water," Ann. N. Y. Acad. Sci. **204**, 79–99 (1973).

[28] R. Pottel, "Dielectric properties," in *Water, a Comprehensive Treatise: Aqueous Solutions of Simple Electrolytes*, edited by F. Franks (Springer, 1973), Vol. 3, pp. 401–431.

[29] V. H. Sack, "The dielectric constants of solutions of electrolytes at small concentrations," Phys. Z **28**, 199–210 (1927).

[30] J. Hasted, D. Ritson, and C. Collie, "Dielectric properties of aqueous ionic solutions. Parts I and II," J. Chem. Phys. **16**, 1–21 (1948).

[31] E. Glueckauf, "Bulk dielectric constant of aqueous electrolyte solutions," Trans. Faraday Soc. **60**, 1637–1645 (1964).

[32] L. Onsager, "Electric moments of molecules in liquids," J. Am. Chem. Soc. **58**, 1486–1493 (1936).

[33] V. A. Markel, "Introduction to the Maxwell Garnett approximation: Tutorial," J. Opt. Soc. Am. A **33**, 1244–1256 (2016).

[34] U. Kaatze, "The dielectric properties of water in its different states of interaction," J. Solution Chem. **26**, 1049–1112 (1997).

[35] U. Kaatze, "Bound water: Evidence from and implications for the dielectric properties of aqueous solutions," J. Mol. Liq. **162**, 105–112 (2011).

[36] J. Hubbard, L. Onsager, W. Van Beek, and M. Mandel, "Kinetic polarization deficiency in electrolyte solutions," Proc. Natl. Acad. Sci. U. S. A. **74**, 401–404 (1977).

[37] J. Hubbard, "Kinetic dielectric decrements and conducting liquids," Biosystems **8**, 201–205 (1977).

[38] K. Tielrooij, R. Timmer, H. Bakker, and M. Bonn, "Structure dynamics of the proton in liquid water probed with terahertz time-domain spectroscopy," Phys. Rev. Lett. **102**, 198303 (2009).

[39] M. Sega, S. Kantorovich, and A. Arnold, "Kinetic dielectric decrement revisited: Phenomenology of finite ion concentrations," Phys. Chem. Chem. Phys. **17**, 130–133 (2015).

[40] M. R. Wright, in *An Introduction to Aqueous Electrolyte Solutions* (John Wiley & Sons, 2007), Chap. 12.

[41] W. M. Haynes, *CRC Handbook of Chemistry and Physics* (CRC Press, 2014).

[42] A. L. Horvath, *Handbook of Aqueous Electrolyte Solutions* (Halsted Press, 1985).

[43] R. B. McCleskey, D. K. Nordstrom, and J. N. Ryan, "Comparison of electrical conductivity calculation methods for natural waters," Limnol. Oceanogr.: Methods **10**, 952–967 (2012).

[44] B. A. Zimmerman and A. L. Kaleita, "Electrical conductivity of agricultural drainage water in Iowa," Appl. Eng. Agric. **33**, 369 (2017).

[45] A. Gorji, "Precision radio-frequency and microwave dielectric spectroscopy and characterization of ionic aqueous solutions," Ph.D. dissertation (Iowa State University, Ames, IA, USA, 2018).

[46] R. Mancinelli, A. Botti, F. Bruni, M. Ricci, and A. Soper, "Perturbation of water structure due to monovalent ions in solution," Phys. Chem. Chem. Phys. **9**, 2959–2967 (2007).

[47]A. B. Pribil, T. S. Hofer, B. R. Randolf, and B. M. Rode, "Structure and dynamics of phosphate ion in aqueous solution: An *ab initio* QMCF MD study," J. Comput. Chem. **29**, 2330–2334 (2008).
[48]E. Cavell, P. Knight, and M. Sheikh, "Dielectric relaxation in non aqueous solutions. Part 2.—Solutions of tri (*n*-butyl) ammonium picrate and iodide in polar solvents," Trans. Faraday Soc. **67**, 2225–2233 (1971).
[49]J. Barthel, H. Hetzenauer, and R. Buchner, "Dielectric relaxation of aqueous electrolyte solutions. I. Solvent relaxation of 1:2, 2:1, and 2:2 electrolyte solutions," Ber. Bunsengesellschaft Phys. Chem. **96**, 988–997 (1992).
[50]H. Falkenhagen, *Electrolytes (Theorie der Elektrolyte)* (Oxford University Press, Oxford, 1934).
[51]W. M. van Beek and M. Mandel, "Static relative permittivity of some electrolyte solutions in water and methanol," J. Chem. Soc., Faraday Trans. 1 **74**, 2339–2351 (1977).
[52]A. Chandra and B. Bagchi, "Frequency dependence of ionic conductivity of electrolyte solutions," J. Chem. Phys. **112**, 1876–1886 (2000).
[53]T. Yamaguchi, T. Matsuoka, and S. Koda, "A theoretical study on the frequency-dependent electric conductivity of electrolyte solutions," J. Chem. Phys. **127**, 234501 (2007).
[54]J. Anderson, "The Debye-Falkenhagen effect: Experimental fact or friction?," J. Non-Cryst. Solids **172-174**, 1190–1194 (1994).
[55]N. Gavish and K. Promislow, "Dependence of the dielectric constant of electrolyte solutions on ionic concentration: A microfield approach," Phys. Rev. E **94**, 012611 (2016).
[56]V. Navarkhele, R. Agrawal, and M. Kurtadikar, "Dielectric properties of electrolytic solutions," Pramana **51**, 511–518 (1998).
[57]P. Winsor and R. H. Cole, "Dielectric behavior of aqueous sodium chloride solutions," J. Phys. Chem. **89**, 3775–3776 (1985).
[58]S. Schrödle, W. W. Rudolph, G. Hefter, and R. Buchner, "Ion association and hydration in 3:2 electrolyte solutions by dielectric spectroscopy: Aluminum sulfate," Geochim. Cosmochim. Acta **71**, 5287–5300 (2007).
[59]A. Eiberweiser and R. Buchner, "Ion-pair or ion-cloud relaxation? On the origin of small-amplitude low-frequency relaxations of weakly associating aqueous electrolytes," J. Mol. Liq. **176**, 52–59 (2012).
[60]R. Buchner, C. Hölzl, J. Stauber, and J. Barthel, "Dielectric spectroscopy of ion-pairing and hydration in aqueous tetra-*n*-alkylammonium halide solutions," Phys. Chem. Chem. Phys. **4**, 2169–2179 (2002).
[61]H. S. Frank and W.-Y. Wen, "Ion-solvent interaction. Structural aspects of ion-solvent interaction in aqueous solutions: A suggested picture of water structure," Discuss. Faraday Soc. **24**, 133–140 (1957).
[62]K. Ibuki and M. Nakahara, "Effect of relaxation of ionic atmosphere on the short-time dynamics of diffusion-controlled reaction," J. Chem. Phys. **92**, 7323–7329 (1990).